Thermal Distortion Behavior of Graphite Reinforced Aluminum Space Structures

D. G. Zimcik*
Canadian Space Agency, Ottawa, Canada
and
B. M. Koike†
Composite Tecnologia, Sao Paulo, Brazil

The thermal distortion of graphite-reinforced aluminum space structures is evaluated and compared to the performance of graphite/epoxy. Both the coefficient of thermal expansion (CTE) and the thermal conductivity of the material (k) are considered in predicting the final distortion experienced in a typical hostile space environment. The analysis introduces the concept of the total thermal distortion coefficient (TTDC), which enables the optimization of laminate ply configuration for minimum thermal distortion. Using TTDC parameters, parametric design curves for optimized laminate configurations were generated that were not necessarily quasi-isotropic for minimum thermal distortion performance. Graphite/aluminum metal matrix laminates showed minimum TTDC values to be constant with stacking angle ($\pm\theta$), which allows designers to satisfy stiffness or strength requirements with no thermal distortion penalty. A design approach is presented that uses the TTDC coefficient to optimize material mechanical properties with minimum thermal distortion. Finally, a representative example of a large (15 × 1.5 m) slotted waveguide planar array synthetic aperture radar (SAR) antenna, similar to that baselined for the Canadian RADARSAT remote sensing satellite, was chosen to illustrate the application of the design approach.

Nomenclature

E_{11} = modulus of elasticity (fiber direction)
E_{22} = modulus of elasticity (transverse direction)
E_{12} = shear modulus
k = coefficient of thermal conductivity
m = number of θ-deg plies
n = number of zero-deg plies
q = heat flux
r = radius of curvature
T = temperature
T_0 = reference temperature
t = laminate thickness
W = plate width
α = coefficient of thermal expansion (CTE)
α_{11} = CTE (fiber direction)
α_{22} = CTE (transverse direction)
α_s = solar absorptance
ν = Poisson's ratio
θ = ply angle
ρ = out-of-plane curvature
η_M = maximum in-plane width distortion
δ_M = maximum out-of-plane tip distortion
ϵ = thermal emittance
σ = Boltzman's constant

Introduction

THE use of graphite-reinforced aluminum has been considered for fabrication of space structures particularly where very tight thermal distortion requirements associated with high mechanical performance are to be met. In particular, applications include structural hardware and instrument components such as reflector antennas and planar arrays. When compared to polymer-based composites such as graphite-reinforced epoxy, this material has the advantage of better electrical and thermal conductivity[1] and lower susceptibility to space environmental effects.[2,3]

Most past works in the area of thermal distortion resistance consider only the thermal coefficient of expansion in selecting material configurations.[4-6] This approach has merit for steady-state or uniformly heated situations. However, in a space environment the temperature distribution in a structure is often time varying or nonuniform due to radiant heating. For example, radiating heating on one side of a structure as typically occurs with a geostationary satellite may result in a slowly varying or quasi-steady-state temperature distribution throughout the structure. Alternately, a satellite in a day-night low Earth orbit with alternating eclipse and sun exposure will experience transient heating in addition to temperature gradients. Consequently, temperature distribution in the structure plays a large role in determining thermal distortions.

The present analysis evaluates the thermal distortion of particular examples of graphite-reinforced aluminum (P100/6061 and P55/6061) and compares the performance to graphite/epoxy (HMS/5208). In this analysis, both the coefficient of thermal expansion (CTE) and the thermal conductivity of the material (k) are considered in predicting the final distortion experienced in a typical hostile space environment.

The analysis was done in three parts. The first part analyzed the in-plane distortion performance of the materials in a laminated plate, where the thermal distortion requirements for both principal directions are equally important; in other words, where a certain distortion in either of the main directions would affect the structural performance to the same extent. The second part compared the out-of-plane thermal distortion of a plate with an aspect ratio close to one, where the distortions along either principal direction have the same effect on the application performance. The third part compared the materials in a specific application of a waveguide beam as might be used for a radar antenna. A new design approach for this type of element is presented in this part,

Presented as Paper 89-1228 at the AIAA/ASME/AHS/ASC Structures, Structural Dynamics, and Materials Conference, Mobile, AL, April 3-5, 1989; received Mar. 1, 1989; revision received Aug. 1, 1989.

*Payload Manager, RADARSAT Project Technical Office. Member AIAA.
‡Director of Development Composite Technology.

which utilizes the unique properties of the metal matrix composite.

Analysis Approach

Both the CTE and the thermal conductivity of the material (k) are considered in predicting the final thermal distortion experienced by a structure in a typical hostile space environment. The thermal response characteristics of the materials were evaluated by use of the ratio of CTE (α) to k, (α/k). This ratio gives a measure of the thermal distortion resistance to demonstrate the effectiveness of metal matrix materials in thermal distortion critical applications. A small value of this ratio indicates a material that will experience a lower deformation for a given thermal excursion and is more desirable. The thermal conductivity of the material, k, is an important factor since the thermal gradient in a structure is a function of this property. Thermal distortions are determined by both the thermal coefficient of expansion and the temperature distribution in the material.

For a composite material, the resultant material properties of a laminate are a function of the stacking sequence and angles. It is well known that the CTE of a fiber-reinforced composite material can be tailored over a wide range including negative and zero values. The standard equations[7] governing the resultant CTE of an individual lamina or a more complex laminate are widely known and are not repeated here. Similar equations are available for determination of the thermal conductivity k of a laminate.[7] These equations are used as a basis for this analysis.

Although the use of the ratio of CTE to k has been suggested in the past to compare materials for use in space applications, only homogeneous or unidirectional materials have been evaluated.[8-11] The material tailorability (and variability) of a composite material has hindered a more complete optimization study. In the present paper, the values of CTE and thermal conductivity for the principal directions for the laminated materials were combined to create a new parameter called the total thermal distortion coefficient (TTDC) for both in-plane and out-of-plane situations. This TTDC included changes in both the CTE and k values that result from stacking sequence and ply angle changes in the material.

Using this coefficient, in-plane distortions are shown to be of most interest to structures where the thermal distortion in both principal directions of a laminated structure are equally important such as for reflector antennas or planar arrays. Out-of-plane distortions are shown to be of most interest to bending-type structures such as structural beams or struts.

Laminate Plate In-plane Thermal Distortion

Initial Considerations

In the first part of the analysis, laminated plates with symmetric and balanced ply configurations, and with a requirement of minimum in-plane thermal distortion for better performance, were analyzed. The thermal distortions in either of longitudinal x or transverse y directions will affect the performance of the component in a similar manner. The analysis considered laminates with $(\pm\theta, 0_n, \mp\theta)$ ply distribution. It was assumed that a realistic tolerance on ply angle was ± 1 deg.

To compare the materials and optimize the thermal distortion characteristics of the laminate in a global way, or, in other words, in both x and y directions simultaneously, the behavior of the plate was measured in this analysis by the total thermal in-plane distortion coefficient (TTIDC), defined as

$$\text{TTIDC} = \left|\frac{\alpha_x}{k_x}\right| + \left|\frac{\alpha_y}{k_y}\right| \tag{1}$$

The form of the TTDC was chosen to be an extension of the algebraic expression that occurs in the one-dimensional equation of thermal distortion for a beam described later in the paper. The analysis assumed that identical components fabricated from each of the materials were exposed to radiation heating in space due to the sun. It was further assumed that all components had similar external surface thermal-optical properties. It is necessary to apply a surface treatment to graphite/epoxy used in space antenna-type structures to improve the radio frequency (RF) radiating properties and to give better thermal and electrical conductivity characteristics. Also, recent studies have shown that certain materials, particularly those of a polymeric base are greatly affected by exposure to atomic oxygen even for a short term at the low Earth orbit region environment. Therefore a surface treatment is also required for protection purposes. It is assumed that this was provided by metallic coating or plating. Such treatment will give the graphite/epoxy laminate radiating properties that are similar to the graphite/aluminum. Accordingly, both laminates would experience similar heat flux under a given exposure condition to the sun. Heat absorbed and emitted by components made of all materials was therefore equal for equal exposure conditions although internal temperature distributions were not necessarily equal. The material properties used in the analysis are shown in Table 1.

Results and Comments

The optimization process was done using two parameters: the ply angle θ and the number of 0-deg plies. Included in this evaluation was the investigation of the effect of adding 0-deg plies to a $\pm\theta$ cross-ply laminate to improve thermal distortion resistance. A number "n" of 0-deg plies were added to the middle of four-ply, balanced, and symmetric-ply distributions to obtain $(\pm\theta, 0_n, \mp\theta)$ laminates.

Calculated values of TTIDC for each material with several ply angle configurations and different numbers of 0-deg layers are shown in Fig. 1. The angles that will optimize the laminates to give the minimum TTIDC value for the material can also be seen in these curves. It is interesting to note that the minimum TTIDC value for each material remains constant for all optimum θ angle configurations from $n = 0$ to $n = 4$. However, for $n > 4$, the TTIDC increases. Therefore, adding 0-deg plies to a laminate and optimizing the ply angle will not improve the TTIDC. However, adding 0-deg plies can change material stiffness and shear modulus. This allows design flexibility to meet stiffness requirements for a minimum distortion configuration.

The curve in Fig. 2 gives the optimum angles for different number of 0-deg layers in the laminates. This curve is the same for all three materials. The curve stops at $n = 4$ because for greater n values the minimum TTIDC values will increase. The minimum TTIDC value for each material occurs at the configurations where

$$\frac{\alpha_x}{k_x} = \frac{\alpha_y}{k_y} \tag{2}$$

Also, stiffness and shear modulus are equal for both x and y directions ($E_x = E_y$, $E_{xy} = E_{yx}$); although the laminates are

Table 1 Material Properties

Property	Graphite/Epoxy	P100/6061	P55/6061
α_{11} (10^{-5} K^{-1})	−0.080	0.086	0.307
α_{22} (10^{-5} K^{-1})	3.67	2.30	2.40
k_{11} (W/m K)	54.0	240.0	98.0
k_{22} (W/m K)	0.7	193.0	98.0
ν_{12}	0.21	0.4	0.27
ν_{21}	0.010	0.031	0.041
E_{11} (10^6 psi)	24.97	51.0	30.8
E_{22} (10^6 psi)	1.17	4.0	4.7
E_{12} (10^6 psi)	0.62	2.0	1.9

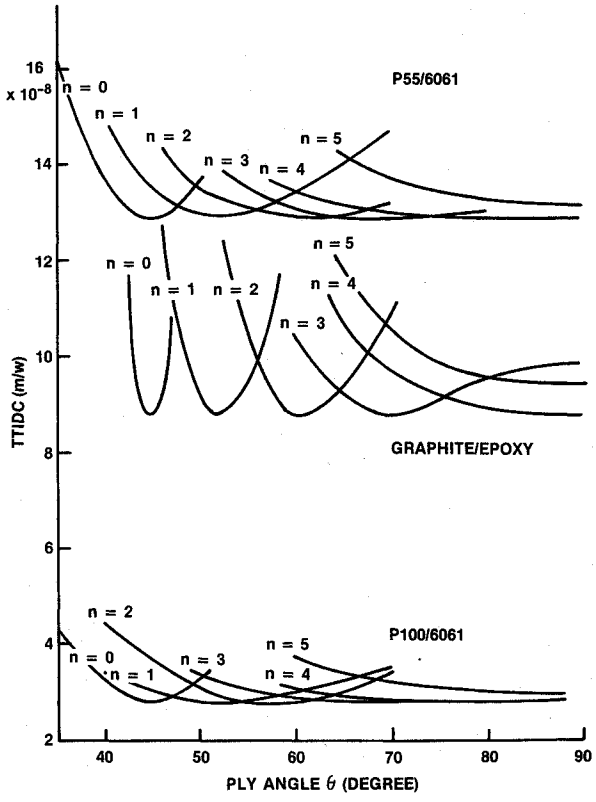

Fig. 1 Calculated TTIDC values for material performance comparison.

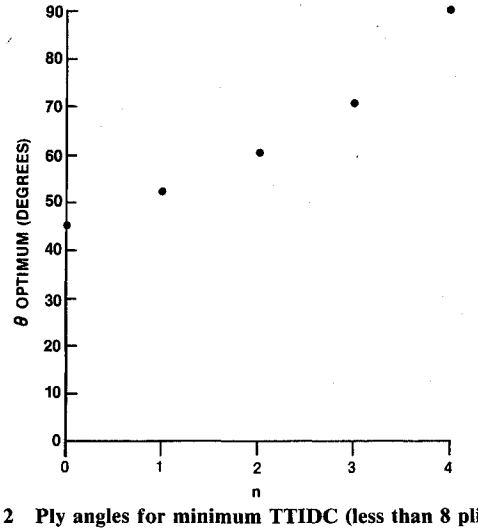

Fig. 2 Ply angles for minimum TTIDC (less than 8 plies).

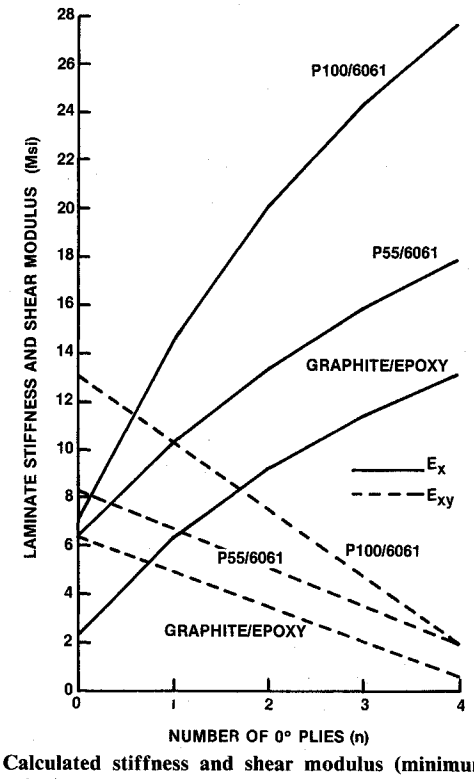

Fig. 3 Calculated stiffness and shear modulus (minimum TTIDC configuration).

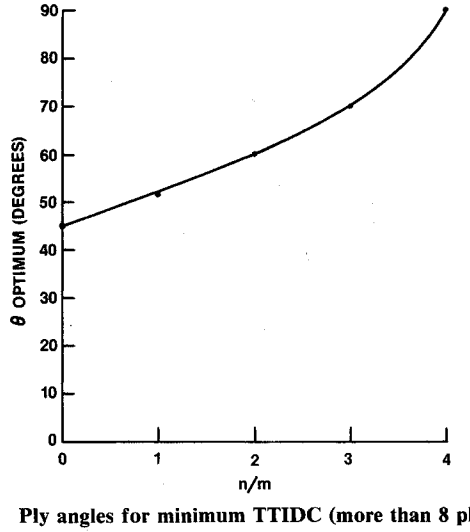

Fig. 4 Ply angles for minimum TTIDC (more than 8 plies).

not generally quasi-isotropic. Figure 3 shows the laminate stiffness and shear modulus for the optimum angle configurations for the subject materials.

These curves do not represent straight lines, as expected, due to the 1-deg quantization approach for the calculations. An optimized 4-layer laminate can have either a maximum stiffness configuration, $(90, 0)_s$ or a maximum shear modulus configuration, $(\pm 45)_s$. Although it could appear that the $(90, 0)_s$, does not fit the initially assumed general laminate configuration $(\pm\theta, 0_n, \mp\theta)$, it is considered here because it is equal to the $(\pm 90, 0_n, \mp 90)$ laminate.

The results show that for more than four 0-deg plies, the TTIDC will increase. More correctly, if more than half of the laminate consists of 0-deg plies, the TTIDC will increase with the addition of extra 0-deg plies. Therefore, if a thicker laminate is required for thermal distortion resistance, it could be obtained as a multiple of the $(\pm\theta, 0_n, \mp\theta)$ configuration, i.e., $(\pm\theta_m, 0_n, \mp\theta_m)$. In this case the curve of Fig. 2 assumes the form of a continuous line. The optimum angle θ will be a function of (n/m) as shown in Fig. 4.

To calculate n and m for a desired laminate of I number of plies, it is necessary to observe

$$(n/m) \leq 4 \tag{3}$$

$$4m + n = I \tag{4}$$

These relations will give $[(I/4) - 1]$ possible configurations for the laminate with minimum TTIDC value. The configuration choice can then be optimized for the desired stiffness and shear modulus characteristics.

As an example, if an $I = 13$ ply laminate with minimum TTIDC is desired, there would be $[(13/4) - 1] = 2$ possible

configurations. These are

$$m = 2, \quad n = 5, \quad (n/m) = 2.5 \tag{5}$$

and

$$m = 3, \quad n = 1, \quad (n/m) = 0.33 \tag{6}$$

the optimum angles θ_{0p} for minimum TTIDC can be found in Fig. 4 as

$$(n/m) = 2.5 \rightarrow \theta_{0p} \approx 65 \text{ deg} \tag{7a}$$

$$(n/m) = 0.33 \rightarrow \theta_{0p} \approx 47 \text{ deg} \tag{7b}$$

Although both configurations represent a minimum thermal distortion configuration, each has different stiffness performance.

Out-of-Plane Distortion

Initial Considerations

The second part of the analysis considered a hollow bending type component, with an aspect ratio close to one, made with a symmetric and balanced ply configuration where minimum out-of-plane thermal distortion was required. The out-of-plane thermal distortions in either the longitudinal x or transverse y directions will affect the performance of the component in a similar manner. An example of such an application would be a planar array antenna where the operational efficiency, as measured by gain or phase distortions, is very sensitive to out-of-plane bending in either direction. The analysis considered laminates with $(\pm\theta, 0_n, \mp\theta)$ ply distribution.

For a given geometry and set of conditions, the out-of-plane distortion can be evaluated using the ratio α/k as described earlier. To optimize for distortions in both x and y directions simultaneously, the behavior of the component was measured by the total thermal out-of-plane distortion coefficient (TTODC) defined as

$$\text{TTODC} = \frac{|\alpha_x| + |\alpha_y|}{k_y} \tag{8}$$

This parameter is similar to the earlier TTIDC, but only the transverse conductivity k_y is included to evaluate out-of-plane bending. The structure modeled is a hollow, closed section with isothermal face sheets as shown in the sketch in Fig. 5. Although the hollow core may be filled with a low effective conductivity material such as honeycomb, the external skin constitutes the major heat conducting path. An antenna reflector or planar array, of sandwich construction, in geostationary orbit with sun on one side and deep space on the other would be a typical example. Similar considerations described previously relating to exterior surface treatment are applicable here. Therefore the thermal radiative properties for the graphite/epoxy and graphite/aluminum plates are considered similar.

Results and Comments

TTODC values were calculated with varying ply angle configurations and different numbers of 0-deg layers. The results are presented graphically in Fig. 6, which shows the angles that give the minimum TTODC value for the plates. For the graphite/aluminum, P100/6061 and P55/6061, the resulting curves of TTODC vs θ were very similar to those obtained in the first part of this analysis. This is explained by the similar values for thermal conductivity in the main directions, x and y, presented by these materials. The minimum TTODC for these materials again remained constant for laminates with zero to four 0-deg plies but increased for $n > 4$. The optimum TTODC occurred at configurations where $\alpha_x = \alpha_y$.

The graphite/epoxy, however, presented thermal conductivity coefficients with quite different values in the x and y directions. Therefore, the minimum TTODC values no longer occurred where $\alpha_x = \alpha_y$ and distortions in x and y directions were different. The TTODC minimum values were different for different numbers of 0-deg. plies in the laminate. Also, at the minimum TTODC configuration, the graphite/epoxy will present a greater distortion in the x-direction than the transverse one.

The optimum θ angle values for the corresponding number of 0-deg plies in the laminate for the graphite/aluminum are the same as shown in Fig. 4. Corresponding values for graphite/epoxy laminates are shown in Fig. 7. Similar to the laminate in-plane distortion, the minimum TTODC values will increase for more than four 0-deg plies for all materials. The same consideration discussed earlier is applicable for laminates thicker than 8 layers, using the $(\pm\theta, 0_n, \mp\theta)$ configuration.

Variation of stiffness and shear modulus with the number of 0-deg layers for the three subject materials is shown in Fig. 8. Small deviations from the straight lines are attributed to the one-deg quantization approach for these calculations. The optimized 4-layer laminate can have either a maximum stiffness configuration $(90, 0)_s$ or a maximum shear modulus configuration $(\pm 45)_s$ for the graphite/aluminum or $(\pm 46)_s$ for the graphite/epoxy.

Design Procedure

It is possible, by the use of the previous curves, to design a component optimized for out-of-plane thermal distortion.

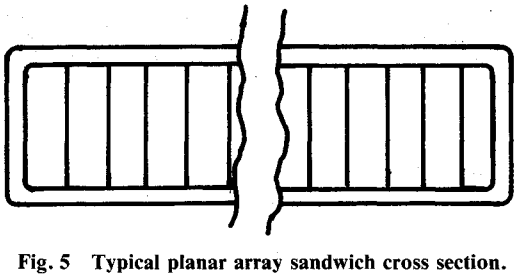

Fig. 5 Typical planar array sandwich cross section.

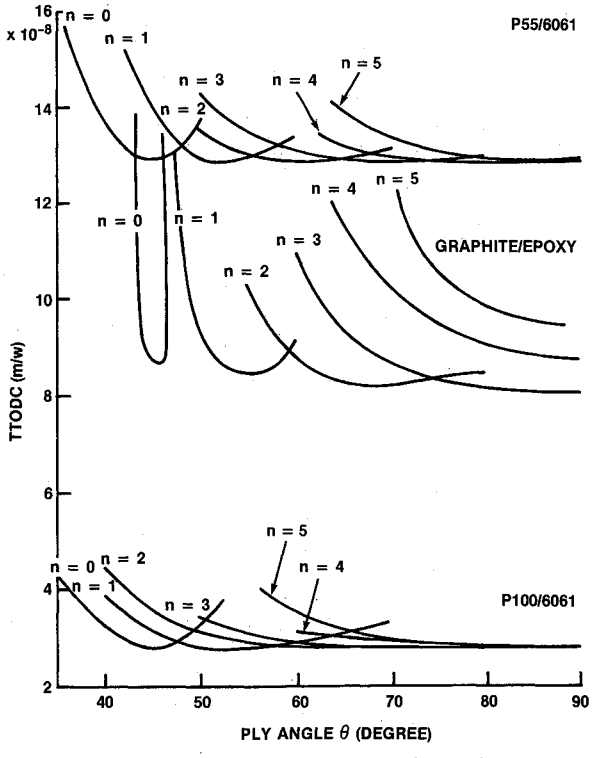

Fig. 6 Calculated TTODC values for material performance comparison.

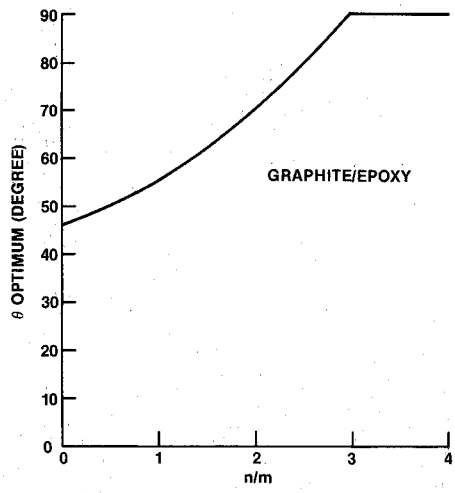

Fig. 7 Ply angles for minimum TTODC for graphite/epoxy.

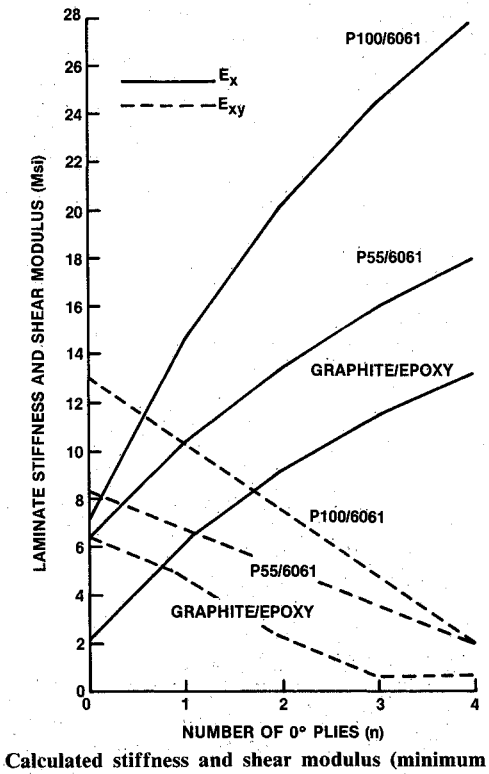

Fig. 8 Calculated stiffness and shear modulus (minimum TTODC configuration).

The suggested procedure is as follows: 1) establish the maximum thermal distortion allowed to size the material thickness, 2) calculate the different possible configurations of the laminate (i.e., n and m), 3) choose the best laminate configuration based on relevant mechanical properties, for example the stiffness and shear modulus, which could be done using Fig. 3 or 8, and 4) once the best configuration is selected, find the corresponding θ angle by using the curves in Fig. 4 or 7. It is interesting to note that the end result of this optimizing procedure will not generally be a quasi-isotropic configuration.

Planar Array Application

To illustrate the application of the design approach, a representative example of a large (15 × 1.5 m) slotted waveguide planar array synthetic aperture radar (SAR) antenna, similar to that baselined for the Canadian RADARSAT remote sensing satellite, was chosen. The RADARSAT satellite will be placed into a near-polar low Earth orbit, which will include periods of eclipse for the antenna structure resulting in transient radiating heating. Planarity of the SAR antenna is critical to performance of the radar. Comparison of out-of-plane bending resulting in tip distortion for each of the candidate materials was conducted, and the results are presented below.

The design of the planar array antenna uses slotted waveguide radiators running the length of the long dimension of the antenna. Accordingly, each waveguide represents a high aspect ratio, rectangular cross-section member with stringent out-of-plane distortion requirements.

Although an analysis similar to the one described in the last section could be completed, the approach can be simplified due to the high aspect ratio of the component to be modeled. Only the out-of-plane distortion in the long direction will be shown to be significant in the following development.

The SAR antenna can be modeled as a series of parallel box beams with flanges separated by parallel webs of width w. Each of these box beams is similar in cross section to that shown in Fig. 5. Neglecting shadowing effects and material variation, each beam will react in the same manner and can therefore be treated individually. For steady-state heat flow, the curvature will be constant over the length of the beam. The thermally induced curvature in the beam for small deflections can be determined, based on the following equation.[12]

$$\rho_i = \left(\frac{\alpha_i}{k_y}\right) + \left(\frac{(W/w)q}{1 + \alpha_i(T_i - T_0)}\right) \tag{9}$$

where

ρ_i = curvature along i axis
α_i = CTE in i direction
W = beam flange width
w = beam web thickness
k_y = conductivity through the web

This expression assumes that the top and bottom surfaces of the component are isothermal and that a linear temperature distribution exists from the top surface temperature T_1 to the bottom surface at temperature T_2 in a steady-state condition.

Requirements

Typical requirements for each waveguide element of the RADARSAT SAR antenna are

1) maximum tip distortion: $\delta_M = 1.75$ mm,
2) maximum width distortion: $\eta_M = \pm 0.08$ mm, and
3) minimum weight.

The material properties are those shown in Table 1. Identical thermal-optical surface properties are assumed for the graphite/aluminum and for the metallic coated graphite/epoxy. Therefore, the temperature variation for a given situation is the same for both materials. Material properties are 1) emittance $\epsilon = 0.06$ and solar absorptance $\alpha_s = 0.3$.

The absorbed heat is given by

$$q = (\alpha_s \cdot s)/2 \tag{10}$$

where s (sun energy flux) = 1350 W/m^2

$$q = 202.5 \text{ W/m}^2$$

As a first approximation,

$$T_1 \approx T_2 = q/\sigma\epsilon, \qquad T_2 = 493 \text{ K} \tag{11}$$

Temperature variation across the array thickness is given by $\Delta T = T_2 - T_0$ where T_0 (initial temperature) = 293 K. This yields a temperature difference

$$\Delta T = 200 \text{ K}$$

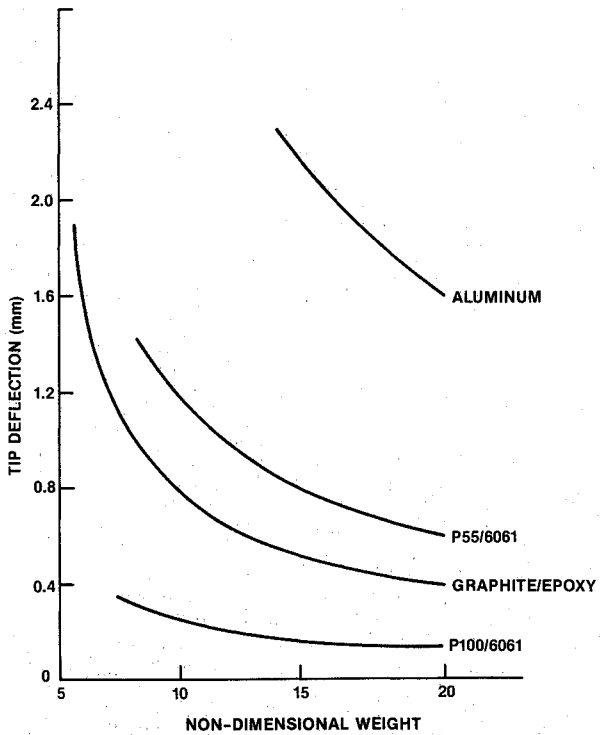

Fig. 9 Thermally induced tip distortion (planar array antenna).

Maximum α_y Calculation

The maximum width distortion requirement gives an upper limit for the allowable value of α_y

$$\alpha_{yM} = \frac{\eta_M}{\Delta T(W)} \tag{12}$$

$$\alpha_{yM} \simeq 1.1 \times 10^{-5}\ \mathrm{K}^1 \tag{13}$$

Even for these very large temperature excursions, either material can meet the tight engineering tolerances allowed for the maximum lateral expansion of the waveguide. Therefore, the problem can be reduced to a single one-dimensional beam bending problem.

Distortion Calculation

The tip distortion can be determined from simple geometry knowing the beam curvature. Values of tip distortion were calculated for several laminate configurations for the three materials. The results are presented in Fig. 9 as a function of a nondimensional weight parameter. It is important to note that neither the metal matrix laminate nor the graphite/epoxy were optimized at a quasi-isotropic configuration as one might initially expect. It is possible to improve the laminate characteristics and get much better properties than the quasi-isotropic laminate for the design of this type of component.

Conclusions

The present analysis introduces the concept of total thermal distortion coefficient (TTDC), which enables the optimization of laminate ply configuration for minimum thermal distortion. The analysis considered laminates in components that were exposed to radiation heating in space due to sun exposure. By using TTDC parameters, the analysis generated parametric design curves for optimized laminate configurations for minimum thermal distortion performance. Graphite/aluminum metal matrix laminates showed minimum TTDC values to be constant with stacking angle ($\pm\theta$). Adding 0-deg plies to a laminate will not improve the TTDC; however adding the plies did change other mechanical parameters such as stiffness and shear modulus. This allows design flexibility to meet stiffness requirements for a minimum distortion configuration. Minimization of in-plane thermal deformations resulted in laminates where $\alpha_x = \alpha_y$ for both metal and polymer matrix materials, but minimization of out-of-plane thermal deformations for graphite/epoxy no longer occurred for laminates where $\alpha_x = \alpha_y$ due to the differing thermal conductivity in the principal directions. Although TTODC for graphite/epoxy did decrease slightly for increasing number of 0-deg plies up to four, the change was not large. Finally, a design approach is presented that uses the TTDC coefficient to optimize material mechanical properties with minimum thermal distortion. The metal matrix composite showed superior performance over the graphite/epoxy material for all cases analyzed in this work.

References

[1]Schulz, D. A., "Production and Properties of Ultra-High Modulus Pitch-Based Carbon Fibers," *Proceedings of the Sixth Metal Matrix Composites Technology Conference,* MMCIAC, Kaman Tempo, Santa Barbara, CA, May 1985, pp. 29-1 to 29-14.

[2]Zimcik, D. G., and Maag, C. R., "Results of Apparent Atomic Oxygen Reactions with Spacecraft Materials During Shuttle Flight STS-41G," *Journal of Spacecraft and Rockets,* Vol. 25, No. 2, 1988, pp. 162–168.

[3]Tennyson, R. C., and Zimcik, D. G., "Space Environment Effects on Polymer Matrix Composite Structures," *Proceedings CNES, ESA & CERT International Symposium on Spacecraft in Space Environment,* ESA SP-178, Toulouse, France, June 1982, pp. 215–226.

[4]Tenney, D. R., Sykes, G. F., and Bowles, D. E., "Composite Materials for Space Structures," *Proceedings of the Third European Symposium on Spacecraft Materials in Space Environment,* ESA SP-232, ESTEC, Noordwijk, the Netherlands, Oct. 1985, pp. 9–21.

[5]Strife, J. R., and Nardone, V. C., "Thermal Expansion Behavior of Graphite Fiber Reinforced Metals," *Proceedings of the Sixth Metal Matrix Composites Technology Conference,* MMCIAC, Kaman Tempo, Santa Barbara, CA, May 1985, pp. 21-1 to 21-7.

[6]MacLean, B. J., and Misra, M. S., "Thermo-Mechanical Behavior of Graphite/Magnesium Composites," *Mechanical Behavior of Metal-Matrix Composites,* edited by J. E. Hack, Metallurgical Society of AIME, Warrendale, PA, Feb. 1983.

[7]Halpin, J. C., *Primer on Composite Materials: Analysis,* Technomic, Stamford, CT, 1984.

[8]Rubin, L., "Applications of Metal-Matrix Composites, The Emerging Structural Materials," *SAMPE Journal,* Vol. 15, No. 4, 1979, pp. 4–9.

[9]Armstrong, H. H., "Satellite Applications of Metal-Matrix Composites," *SAMPE Symposium and Exhibition,* Society for the Advancement of Materials and Process Engineering, Covina, CA, Vol. 24, 1979, pp. 1250–1263.

[10]Wade, W. D., and Ellison, A. M., "The Application of Metal-Matrix Composites to Spaceborne Parabolic Antennas," *SAMPE Symposium and Exhibition,* Vol. 24, 1979, pp. 1265–1275.

[11]Dries, G. A., and Tompkins, S. S., "Effects of Thermal Cycling on Graphite-Fiber-Reinforced 6061 Aluminum," NASA TP 2612, Oct. 1986.

[12]McCoy, D. A., and Lloyd, D. J., "Fabrication of Graphite-Fiber-Reinforced Aluminum," *CASI Journal,* Vol. 33, No. 1, 1987, pp. 11–17.

David H. Allen
Associate Editor